Research Square

Preprints are preliminary reports that have not undergone peer review.
They should not be considered conclusive, used to inform clinical practice,
or referenced by the media as validated information.

Preparation of Amide-Type Polyurethane Biomimetic Chain Extenders and Their Application in the Softening Finishing of Functional Textiles

Heng Quan
Wuhan Textile University
Bing Wu
Wuhan Textile University
Qinglin Fu
Wuhan Textile University
Li Xiao
Hubei Daya Biotechnology Co., Ltd.
Zengfeng Wei
zfwei@wtu.edu.cn
Wuhan Textile University
Lijie Ni
Wuhan Textile University

Research Article

Keywords: Catechol group, Mussel-inspired modification, Waterborne polyurethane, Wash-resistant finishing, Fiber-matrix adhesion

Posted Date: November 5th, 2026

DOI: https://doi.org/10.21203/rs.3.rs-10508764/v1

License: This work is licensed under a Creative Commons Attribution 4.0 International License.
Read Full License

Additional Declarations: No competing interests reported.

Preparation of Amide-Type Polyurethane Biomimetic Chain Extenders and Their Application in the Softening Finishing of Functional Textiles

Heng Quan [1,2], Bing Wu [1,2], Qinglin Fu [1], Li Xiao[3], Zengfeng Wei [1,4*], Lijie Ni [1,4*]

(1. Hubei Key Laboratory of Biomass Fibers & Eco-Dyeing & Finishing, Wuhan Textile University, Wuhan 430200, Hubei, China;

2. School of Textile Science and Engineering, Wuhan Textile University, Wuhan 430000, Hubei. China;

3. Wuhan Textile University (Hubei Daya) Graduate Workstation, Jingzhou 434000, Hubei, China;

4. Hubei Key Laboratory for Clean Recycling and Resource Utilization of Waste Fibers, Wuhan Textile University, Wuhan 430200, Hubei, China)

Corresponding author

E-mail addresses: zfwei@wtu.edu.cn (Zengfeng Wei); vistanlj@wtu.edu.cn (Lijie Ni).

Abstract: To overcome the limitations of insufficient fiber adhesion and inadequate wash-fastness associated with traditional silicone softeners, a polyurethane biomimetic chain extender containing catechol group was designed and synthesized. This chain extender was incorporated into the backbone of a polyurethane-modified silicone softener to produce a resin-type silicone softener, which was then used to treat cotton fabrics. The study characterized the chemical structures of the biomimetic chain extender and the softener, evaluated the emulsion stability of the finishing agent, and tested the crease recovery angle, softness, wash-fastness, and surface morphology of the treated fabrics. The results indicate that the biomimetic chain extender significantly enhances the desired performance characteristics of the polyurethane-modified silicone softener: fabrics treated with biomimetic chain extender exhibited a crease recovery angle of 148.5°, a 28.4% increase compared to the sample without; the softness value was reduced from 201.4 mN to 135.4 mN; fabrics treated with the biomimetic chain extender maintained satisfactory softness even after 30 washes. These results indicate that the introduction of the catechol group enhances the softener's adsorption and film-forming properties on the fiber surface. Through strong interfacial bonding, it improves the wash-fastness of the silicone softener as well as the fabric’s softness and wrinkle resistance, providing new insights for the molecular design of long-lasting textile finishing agents.

Keywords: Polyurethane; Biomimetic chain extender; Silicone; Softening treatment;

preparation; Application

1. Introduction

As an important technological factor influencing the hand feel and wearing comfort of textiles, polymeric softeners have attracted considerable research interest in textile printing and dyeing practices[1–3]. Among these, silicone softeners have become one of the most widely used softeners in textile softening treatments due to their ability to impart excellent flexibility, smoothness, and a fluffy, soft hand feel to fabrics. However, due to the lack of clear physical and chemical bonding between traditional silicone softeners and textiles[4,5], they typically exhibit inadequate wash-fastness[6], easy migration, and unstable finishing effects[7]. In particular, their performance characteristics deteriorate significantly under repeated washing or harsh conditions[8], limiting their long-term application in high-end textiles.

To enhance the wash-fastness of silicone softeners and achieve distinctive styling characteristics, researchers have investigated several strategies, such as innovative molecular structure design, active capping, and crosslinking[9].

For example, Lei synthesized polyurethane-modified silicones via a step-growth polymerization process, achieving a distinctive overall fabric style[10]. However, the incorporation of polyurethane segments into the polysiloxane chains disrupts the ordered arrangement of the polysiloxane segments and their methyl groups on the fiber surface, increasing steric hindrance between methyl groups on some silicon atoms. This reduces the softness and smoothness imparted by the agent. Furthermore, the hydrophobic, flexible polysiloxane segments tend to phase-separate from the hydrophilic, highly elastic polyurethane segments; this microphase incompatibility compromises the consistency of the finishing performance.

Wu[11] first synthesized the hydroxy silane coupling agent KHS using KH121 and KH560, then reacted it thoroughly with a polyurethane prepolymer, and finally added hydroxyl-terminated silicone oil to obtain silicone-modified polyurethane. When used for fabric finishing, by the silane coupling agent significantly improved the fabric's softness and elasticity.

Cho[12] used HDI trimer, 1,6-hexanediol, methoxy polyethylene glycol and 3,5-dimethylpyrazole to synthesize the active capped polyurethane. Finally, the active polyurethane was thoroughly mixed with amino silicone oil to produce a polyurethane-silicone softener. The resulting compound exhibits excellent softness and maintains a low coefficient of friction, even after 20 washing cycles.

In summary, polyurethane (PU), due to its high structural design flexibility, excellent film-forming properties, and superior adhesion, provides an ideal platform for

the development of high-performance, durable, and soft finishing agents[13]. Chain extenders, as key components that regulate the microphase structure, mechanical properties, and surface characteristics of PU, directly influence the durability of the finishing layer[14,15] as well as the style and performance of the fabric.

In recent years, drawing inspiration from mussel adhesion mechanisms[16], researchers have discovered that the catechol group possesses strong interfacial bonding capabilities and demonstrates excellent performance in enhancing fabric antibacterial properties[17], durability[18], and interfacial adhesion[19]. For example, Inata modified alginate with catechol and used it as an adhesive material, demonstrating good bonding strength[20]. Xiao synthesized a catechol-functionalized PEG via the reaction of polyethylene glycol diglycidyl ether with dopamine, which was subsequently blended into the electrospinning solution to prepare a hydrophilic PVDF nanofiber membrane. This composite membrane demonstrated strong and reusable adhesive performance[21]. Lou used a horseradish peroxidase (HRP)/H_2O_2 system to catalyze the grafting and polymerization of 2-chloro-4,6-diamino-1,3,5-triazine (a reactive dye intermediate) onto cotton fabrics, as well as the grafting and polymerization of catechol (CA). It was found that the amino groups in the cotton fibers formed covalent bonds with the reactive groups of CA, thereby enhancing their dyeing performance and colorfastness[22].

Inspired by the high bond energy, strong polarity, and structural stability of natural amide bonds, this study designed and synthesized an "amide-type biomimetic polyurethane chain extender." The aim was to enhance the bonding strength between the finishing agent and the fiber through the interfacial reinforcement effect of amide and hydroquinone groups, thereby significantly improving the wash-fastness of the finishing layer. This study investigates the preparation, structural characterization, and application of the biomimetic chain extender in the finishing of cotton fabrics. Particular emphasis was placed on the retention of "hand feel" characteristics, wash-fastness, and related physical properties of the finished fabrics after repeated washing. These findings were compared with those of traditional finishing systems to elucidate the applications and advantages of the polyurethane-based chain extender in achieving "wash-resistant hand feel" and long-lasting functionality.

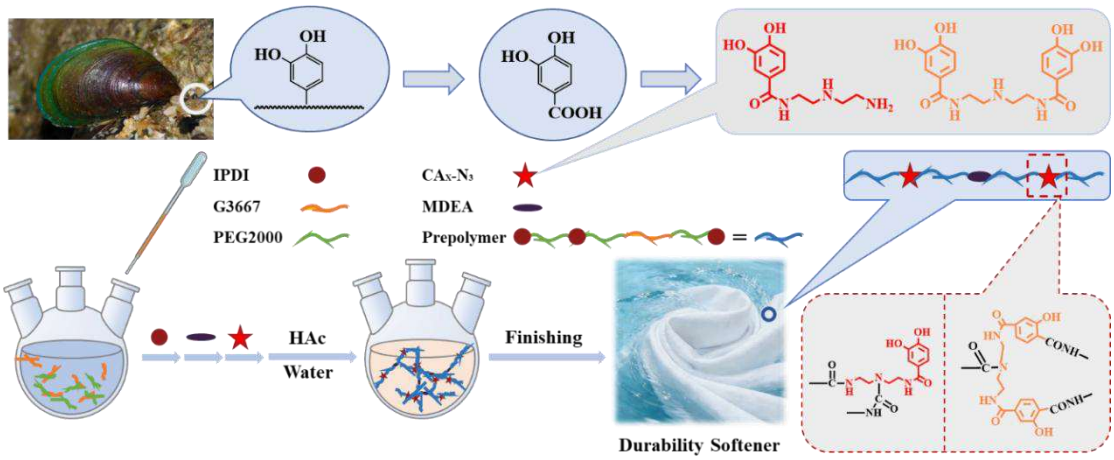


Fig. 1. Synthetic strategy and preparation route

2. Experimental Section

2.1. Materials

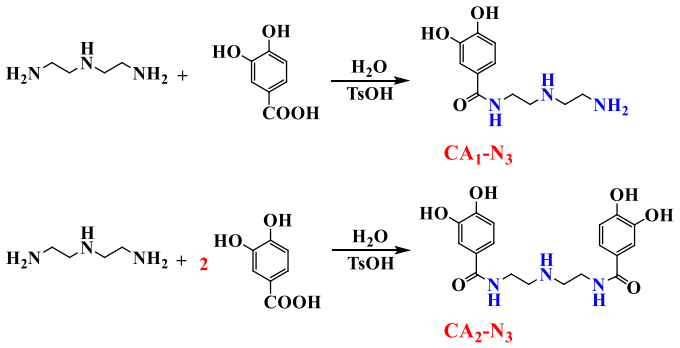
A commercially available knitted cotton fabric (18.5 tex, 100% combed cotton jersey, 270 g/m²) was used. Diethylenetriamine (DETA, 99%), 3,4-dihydroxybenzoic acid (DHB, 99%), p-toluenesulfonic acid (PTS, 99%), dibutyltin dilaurate (DBTDL, 99%), N-methyldiethylamine (MDEA, 99%), N,N-dimethylformamide (DMF, 99%), and glacial acetic acid (HAC, 99%) were all purchased from Shanghai Aladdin Biochemical Technology Co., Ltd. Methyl ethyl ketone (MEK, 99%), ethyl acetate (EAC, 99%), and petroleum ether (PE, 99%) were all purchased from Sinopharm Chemical Reagent Co., Ltd. Isophorone diisocyanate (IPDI, industrial grade) was purchased from Yantai Wanhua Chemical Group Co., Ltd., Shandong, China. Polyethylene glycol 2000 (PEG2000, industrial grade) was purchased from Xuzhou Yihuiyang New Materials Co., Ltd., Jiangsu, China; hydroxyl-terminated silicone oil (G3667, molecular weight 5000, industrial grade) was purchased from Dow Silicones, USA. A resin-type silicone softener (A commercial competitor products supplied by Wuhu Viruan New Materials Co., Ltd.) was also used for performance comparison.

2.2. Preparation of Amide-Type Bionic Polyurethane Chain Extender

2.2.1. Preparation of Catechol-Modified Polyamine (CAx-N3)

The synthetic route for the biomimetic chain extender CAx-N3 is shown in Scheme 1. A predetermined amount of DETA, DHB, and deionized water was added to a three-neck flask equipped with a condenser, a mechanical stirrer, and a nitrogen inlet, and the mixture was reacted at 100 °C for 6 h. During this time, the reaction progress was

monitored by thin-layer chromatography (TLC) until the reaction was complete. Subsequently, the reaction mixture was cooled to room temperature, and the solvent was removed by vacuum distillation. The product was then purified by column chromatography (PE:EAC = 3:7), yielding N-(2-((2-aminoethyl)amino)ethyl) -3,4-dihydroxybenzamide and N,N′-(aziridin-2-ylbis(ethane-2,1-diyl)) bis(3,4-dihydroxybenzamide), which were named CA_1-N_3 and CA_2-N_3, respectively.



Scheme 1. The synthesis routes of CA_x-N_3

N-(2-((2-aminoethyl)amino)ethyl)-3,4-dihydroxybenzamide (CA_1-N_3, yellow oil, 1.7 g, 75%). ^{1}H NMR (400 MHz, DMSO-d6) δ 6.65 (s, 3H), 5.99 (s, 2H), 2.03 (s, 2H), 1.84–1.78 (m, 8H), 1.41 (s, 2H). ^{13}C NMR (100 MHz, DMSO-d6) δ 172.42, 146.14 (t, J = 86.5 Hz), 128.88, 118.33, 50.54, 50.39 (m), 40.45. HRMS (ESI): m/z calcd for $C_{11}H_{17}N_3O_3$ [M+H]+ 239.1263, found 239.1269.

N,N'-(azanediylbis(ethane-2,1-diyl))bis(3,4-dihydroxybenzamide) (CA_2-N_3, yellow oil, 2.96 g, 79%). ^{1}H NMR (400 MHz, DMSO-d6) δ 7.45 (s, 6H), 6.90 (s, 4H), 6.90–6.85 (m, 3H), 2.89 (s, 8H). ^{13}C NMR (100 MHz, DMSO-d6) δ 172.42, 148.58, 129.02 (d, J = 4.9 Hz), 121.25 (dd, J = 512.2, 327.9 Hz), 45.99, 40.08. HRMS (ESI): m/z calcd for $C_{18}H_{21}N_3O_6$ $M^{+\bullet}$ 375.1425, found 375.1426.

2.2.2. Preparation of Polyurethane-Modified Silicone Softener (PUS)

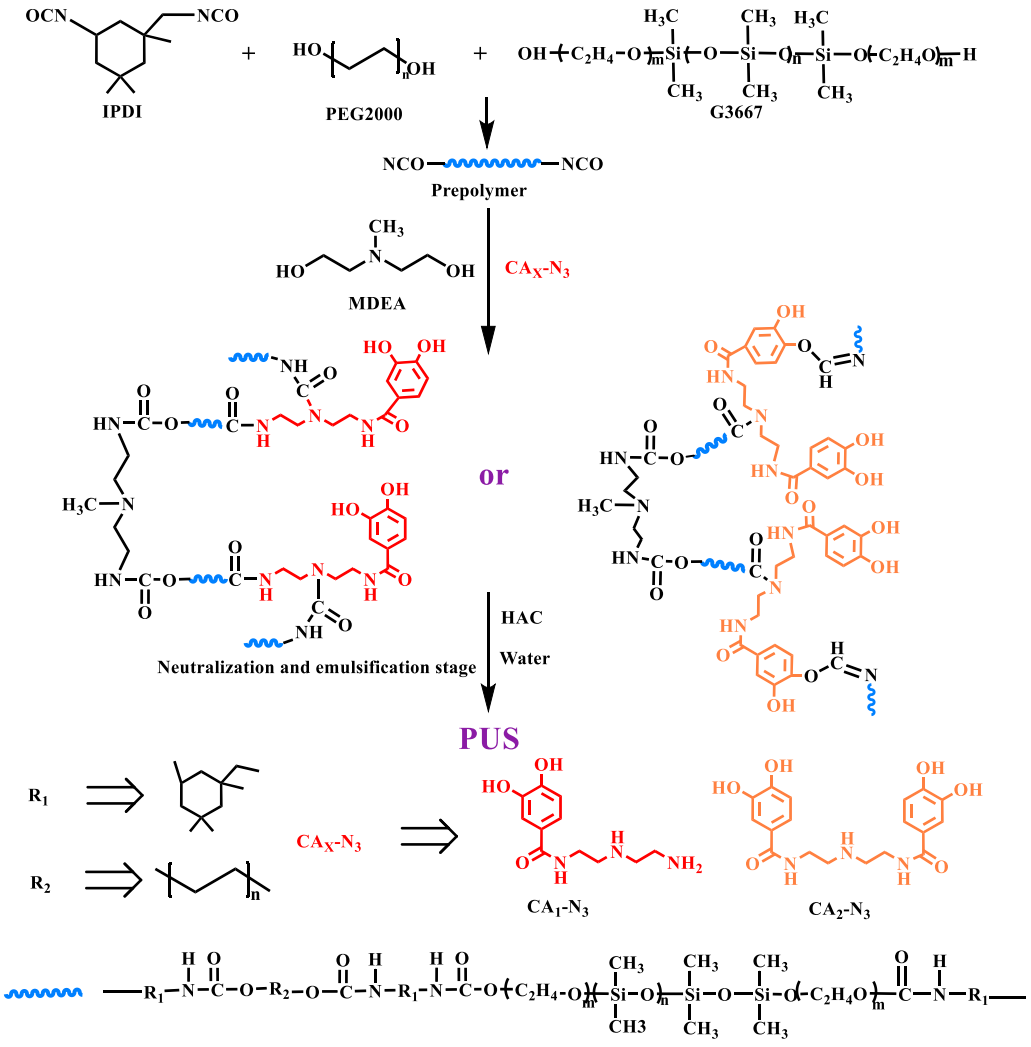
The synthesis process for the silicone softener PUS is shown in Scheme 2. PEG2000 and G3667 were added to a flask and subjected to vacuum dehydration. IPDI diluted with acetone was then added to the flask. The temperature was raised to 85°C, and an appropriate amount of DBTDL was added; the mixture was reacted for 2–3 hours. Subsequently, MDEA diluted with acetone was added to the reaction system at 60°C, reacted for 45 minutes. Afterward, different amount of CA_X-N_3 dissolved in DMF were added dropwise at 60°C for 0.5 h. After the reaction, an appropriate amount of HAC was added to neutralize the mixture at 50 °C for 15 minutes, and deionized water was added dropwise under vigorous stirring to induce emulsification over 30 min.

Finally, the solvent was removed under reduced pressure to obtain the emulsion PUS-Ex-y with a solid content of approximately 20% (The content of CA_X-N_3 is shown in the Table 1).

Table 1. Formulations of polyurethane-modified silicone softeners (PUS) with different biomimetic chain extender dosages

Sample	IPDI(%)	PEG2000(%)	G3667(%)	MDEA(%)	CA_X-N_3(%)
PUS-0	24.5	61.4	11.3	2.8	0
PUS-E1-2	14.2	23.1	57.9	2.8	2
PUS-E1-5	18.1	21.2	52.9	2.8	5
PUS-E1-8	22.3	19.1	47.8	2.8	8
PUS-E2-2	13.3	23.5	58.4	2.8	2
PUS-E2-5	15.7	21.9	54.6	2.8	5
PUS-E2-8	20.9	19.5	48.8	2.8	8

Note: The PUS-E2-8 emulsion sample containing 8% CA_2-N_3 is unstable.



Scheme 2. The synthesis process of PUS

2.3. Structural Characterization and Performance Evaluation

2.3.1. Structural Analysis

Infrared Spectroscopy (FT-IR): Infrared analysis of the samples was performed using a Bruker Tensor 27 Fourier-transform infrared spectrometer; the KBr pellet method was employed, with a measurement range of 4000 cm^{-1} to 500 cm^{-1}.

Nuclear Magnetic Resonance (NMR) Spectra: NMR spectra were recorded using a Varian Mercury Plus 400 MHz NMR spectrometer with $CDCl_3$, CD_3OD, or DMSO-d_6 as solvents. Chemical shifts are reported in parts per million (ppm) relative to tetramethylsilane (TMS)[23].

High-Resolution Mass Spectrometry (HRMS): High-resolution mass spectra were acquired using an Agilent 6530 accurate-mass Q-TOF mass spectrometer.

2.3.2. Emulsion Particle Size and Zeta Potential of Latex Particles

The emulsion samples were characterized using a Malvern NanoZS90 nanoparticle size and zeta potential analyzer from Malvern Instruments Ltd. (UK). The sample to be tested was diluted with water to 1.0 wt.%, sonicated for 20 min to ensure uniform dispersion of the emulsion, and tested at 25°C[24].

2.3.3. Thermal Gravimetric Analysis (TG)

The samples were tested using a Hitachi STA300 thermogravimetric analyzer. Under a nitrogen atmosphere, 3–10 mg of dried sample was placed in a crucible and tested within the temperature range of 30–800 °C at a heating rate of 10 °C/min[25].

2.3.4. Acid and Alkali Stability of the Emulsion

Dilute the emulsion to 10 g/L, and adjust the pH to the desired value within the range of 1–14, using hydrochloric acid for acidic pH or sodium hydroxide for alkaline pH. Shake the emulsion and let it stand for 30 minutes, then observe for any signs of turbidity, phase separation, coating on the walls, or precipitation.

2.3.5. Salt Stability of the Emulsion

Dilute the emulsion to 10 g/L, add 0.2 mL of 1.0 wt.% NaCl solution, and let it stand for 30 minutes. Observe for any signs of turbidity, separation, wall adhesion, or precipitation.

2.3.6. Centrifugation Stability of the Emulsion

Dilute the emulsion to 10 g/L, centrifuge at 4000 rpm for 30 minutes using a TGL-16G bench-top high-speed centrifuge (Shanghai Fichar Analytical Instrument Co., Ltd.). Observe for any signs of cloudiness, separation, residue on the tube walls, or precipitation.

2.3.7. Fabric Performance Testing

Soaked the fabric in PUS emulsion (30 g/L) for 30 seconds, perform a two-dip, two-roll treatment, dry at 100 °C for 5 minutes, and then cure at 150 °C for 3 minutes. Test the finished fabric after equilibrating it for 24 hours under standard conditions (temperature 20 °C, relative humidity 65%).

(1) **Surface Morphology:** Secure the fabric sample to the test stage with conductive adhesive, perform gold sputtering on the sample (accelerating voltage: 20 kV; sputtering time: 60 seconds), and observe the sample morphology using a JEOL JSM-IT500A scanning electron microscope.

(2) **Softness:** Softness was tested using an NW254 Softness Tester (Quanzhou Meibang Instrument Co., Ltd.) in accordance with the GB/T 8942-2016 standard method. Samples were taken along the warp and weft directions of the fabric, and the softness was determined as the arithmetic mean of the two results.

(3) **Crease Recovery Angle**: The YG541E fully automatic laser fabric crease elasticity tester from Ningbo Textile Instrument Factory was used to measure the warp and weft crease recovery angles of the fabric in accordance with GB/T 3819-1997 “Determination of Crease Recovery of Textile Fabrics—Recovery Angle Method.” Three tests were conducted, and the average value was taken.

(4) **Soap Wash Resistance**: Testing was conducted in accordance with GB/T 8629-2017 standard method. The washing temperature was 40 °C with a liquor ratio of 1:50. The fabric was washed 5, 10, and 30 times, with each wash lasting 10 minutes.

3. Results and Discussion

3.1. Structural Analysis

The ^{1}H NMR spectrum of the biomimetic chain extender CA_1-N_3 is shown in Figure 1(a). The chemical shifts of the three aromatic protons on the benzene ring appear at δ 6.65; the two protons of the methylene group attached to the amide bond resonate at δ 2.03; and the eight protons of the long-chain methylene groups appear at δ 1.84–1.78. The signals denoted as c and c* in the spectrum are resolved into two distinct peaks, indicating that the two corresponding species are not fully equivalent.

This confirms that 3,4-dihydroxybenzoic acid reacts preferentially with primary amines over secondary amines.

The ^{1}H NMR spectrum of the biomimetic chain extender CA_2-N_3 is shown in Figure 1(b): the chemical shift of the six aromatic protons on the benzene ring appears at δ 7.45, the chemical shift of the four protons on the two methylene groups linked to the amide bond is at δ 2.89, and the chemical shift of the four protons on the two long-chain methylene groups is at δ 2.74. The presence of only one peak for c in this figure is due to the complete symmetry of the corresponding product formed in the reaction.

The infrared spectrum of the biomimetic chain extender CA_x-N_3 is shown in Figure 1(c): the absorption peaks at 3360 cm^{-1} and 3256 cm^{-1} are both attributed to the O–H stretching vibrations of the phenolic hydroxyl groups in the biomimetic chain extender molecule; the peak at 3280 cm^{-1} in CA_1-N_3 is attributed to the N–H stretching vibration of the primary amine, while the absorption peak at 3045 cm^{-1} in CA_2-N_3 appears as a sharper peak and is attributed to the N–H stretching vibration of its secondary amine; the peaks at 1660 cm^{-1} and 1630 cm^{-1} are both attributed to the stretching vibrations of the C=O bond in the amide group; the peaks at 1500 cm^{-1} and 1475 cm^{-1} are both attributed to the vibrations of the attached benzene ring; the absorption peak of CA_2-N_3 at 1475 cm^{-1} is at a lower wavenumber and has a more complex shape. This discrepancy is due to the difference in the number and position of substituents on the benzene ring compared to CA_1-N_3, which leads to changes in the vibrational modes.

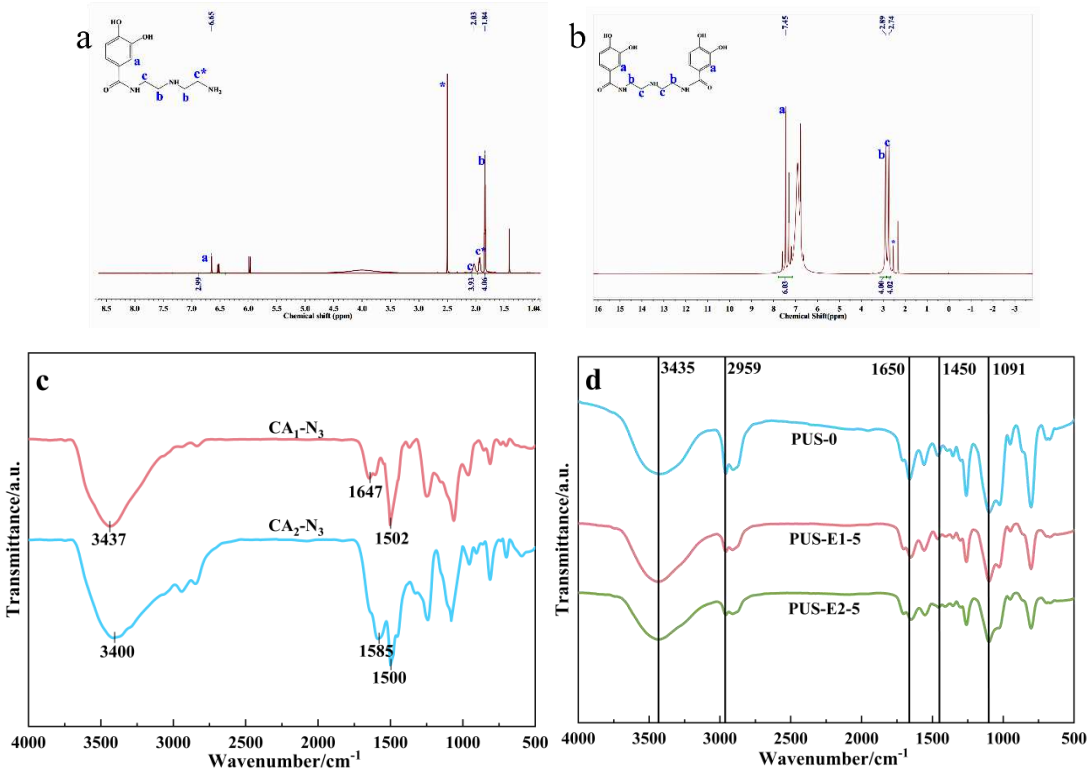


Fig. 2. (a) ^{1}H NMR spectrum of CA_1-N_3; (b) ^{1}H NMR spectrum of CA_2-N_3; (c) FT-IR spectra of biomimetic chain extenders CA_1-N_3 and CA_2-N_3; (d) FT-IR spectra PUS emulsion

Infrared spectroscopy was performed on PUS-0, PUS-E1-5, and PUS-E2-5 as a typical representative. In Figure 1(d), the peak at 3435 cm^{-1} corresponds to the N-H stretching vibration. The peak of PUS-0 is narrower, whereas that of PUS-E1-5 is significantly broader and more intense, due to the overlap between the N-H peak of the carbamate and those of the primary amine and phenolic hydroxyl groups in the latter; PUS-E2-5 exhibits the broadest and strongest peak in this region, owing to its higher content of phenolic hydroxyl and secondary amine groups, which results in a denser intermolecular hydrogen-bonding network. The peak at 2959 cm^{-1} corresponds to the C–H stretching vibration of the carbon chains in the samples. The peak at 1650 cm^{-1} in PUS-0 is attributed to the C=O stretching vibration of the amide group, while the C=O peaks of PUS-E1-5 and PUS-E2-5 shift to approximately 1630 cm^{-1} due to conjugation between the amide bond in the biomimetic chain extender and the benzene ring, which reduces the bond order of the C=O group. The peak at 1450 cm^{-1} in PUS-0 is attributed to the C-H vibration of the isocyanate-derived structure[10,11] ; in the other two samples, the absorption at 1450 cm^{-1} also includes the C=C stretching vibration of the benzene ring from the biomimetic chain extender. The strong peak at 1091 cm^{-1} is assigned to the C–O stretching vibration of the PEG backbone in the PUS samples.

3.2. Thermogravimetric Analysis

As shown in Figures 3(a) and (b), PUS-0 exhibits high stability at elevated temperatures. The weight loss of the sample between 200°C and 400°C is attributed to the thermal degradation of its polymer backbone; specifically, the pyrolysis temperature range for urethane bonds is 200°C to 300°C, and for silyl ethers, it is 300°C to 400°C. This process is accompanied by the thermal degradation of Si-C, C-N[26], C-H[27], and C-C[28] bonds, among others .

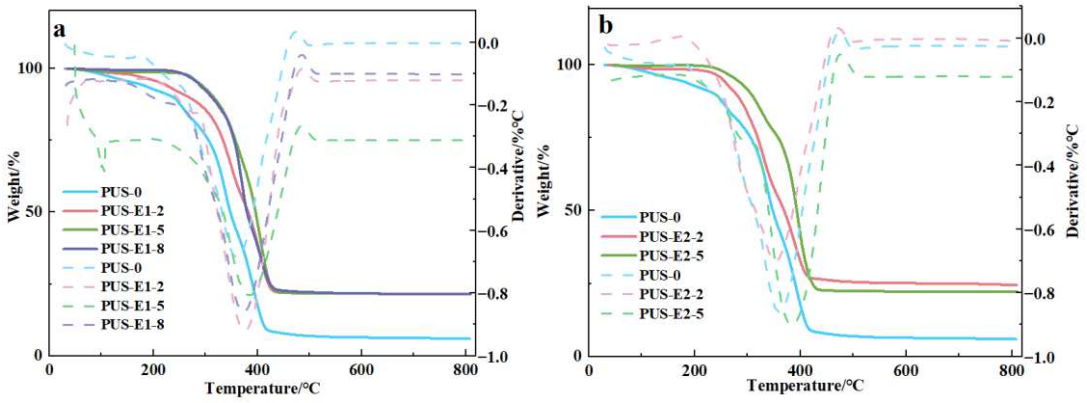


Fig. 3. TG and DTG curves of PUS samples containing (a) CA_1-N_3 and (b) CA_2-N_3 biomimetic

chain extenders at different dosages

In samples containing the same type of biomimetic chain extender, the thermal stability of the product increases with the increasing amount of chain extender; the higher the amount of biomimetic chain extender, the greater the degree of cross-linking in the polymer, and the better its thermal stability. This is because the introduction of the biomimetic chain extender not only increases the rigidity of the molecular chains but may also enhance intermolecular interactions through hydrogen bonding, thereby delaying the thermal transformation process; this modification improves the stability of the samples under high-temperature conditions. Furthermore, the introduction of the biomimetic chain extender results in a higher degree of rigidity in the mixed-aggregate phase of the polymer product, which, to some extent, suppresses the tendency for phase separation, thereby leading to improved thermal stability of the product.

As shown in Figures 3(a) and (b), except for PUS-0, which exhibited a weak two-step thermal degradation (at approximately 270 °C and 370 °C), all other samples displayed essentially a single main weight-loss step between about 250 °C and 400 °C. This can be attributed to two factors. First, in PUS-0, the very low proportion of G3667 segments makes it nearly impossible to form an effective microphase-separated structure with PEG2000. Second, for samples containing biomimetic chain extenders, although the proportions of G3667 and PEG2000 are both high and comparable, the cross-linking effect and rigid structure of the biomimetic chain extenders also suppress the formation of effective microphase separation, both between soft-segment domains and between soft and hard phases.

As the proportion of the biomimetic chain-extender increases, the temperature at which the sample loses 50% of its mass rises from 360°C for PUS-E1-2 to 370°C for PUS-E1-8, indicating improved thermal stability. This is also attributed to the inhibitory effect of the biomimetic chain-extender's cross-linking action and rigid structure on the microphase separation between soft-segment phases and between soft and hard segments.

The TG curves of the samples exhibited two or three subtle thermal weight loss steps. For PUS-0, the steps observed at 175 °C and 339 °C are related to its high moisture content (weight loss below 100 °C) and localized microphase separation (weight loss around 300 °C), respectively, resulting from the lack of sufficient rigid structure. For the samples containing biomimetic chain extenders, these subtle steps are primarily associated with minor localized microphase separation or an uneven cross-linked structure.

The carbon residue content of PUS-0 is approximately 6%, whereas that of the

samples extended with biomimetic chain extenders is about 25%, indicating a significantly higher carbon residue. This is partly due to the higher incorporation ratio of G3667 and partly due to the cross-linking effect of the biomimetic chain extender. However, the cross-linking effect also weakens, to some extent, the contribution of G3667 to the carbon residue, leading to a convergence of the residue content among the different samples.

3.3. Emulsion Stability

Zeta potential measurements were performed on all sample emulsions (Table 2). It can be observed that PUS-0 had the highest average potential among all samples at 43.65 mV, indicating that its emulsion possesses good dispersion stability. Meanwhile, the zeta potentials of the emulsion particles in PUS-E1-2 and PUS-E2-2 ranged between 24.15 and 38.19 mV, also demonstrating excellent colloidal stability[29] . The zeta potential of the samples originates from the cationic chain extenders in the formulation; however, the cross-linking action and rigidity of the biomimetic chain extenders may partially shield the positive charge of the molecules when used in higher concentrations.

Regarding emulsion stability: All emulsion samples remained stable over a wide pH range (pH 4-8), becoming turbid only when the pH exceeded 8 or fell below 4; their excellent salt stability demonstrates that the emulsions can maintain their dispersed state even under high ionic strength; and the centrifugation stability test results indicate that these emulsions possess excellent storage stability. The favorable stability of the emulsions is attributable not only to the cationic groups in their molecular structure but also to their relatively high polyethylene glycol content.

Table 2. Emulsion stability properties of PUS softeners

Sample	Size (nm)	Zeta potential (mV)	pH Stability	Salt Stability	Centrifugal Stability
PUS-0	79.51	43.65	4-8	Clear	Clear
PUS-E1-2	111.67	38.19	4-8	Clear	Clear
PUS-E1-5	189.09	29.11	4-8	Clear	Clear
PUS-E1-8	205.07	26.78	4-8	Clear	Clear
PUS-E2-2	155.13	33.83	4-8	Clear	Clear
PUS-E2-5	258.03	24.15	4-8	Clear	Clear

Note: Due to the unstable emulsion state, PUS-E2-8 has not been listed.

3.4. Fabric Performance Testing

3.4.1. Crease Recovery Angle

As shown in Figure 4, compared to fabrics treated with the sample containing no biomimetic chain-extender (PUS-0), fabrics treated with the sample containing the biomimetic chain-extender exhibited a significantly increased crease recovery angle. Furthermore, as the dosage of the biomimetic chain extender increased, the elasticity of the treated fabrics improved significantly. The crease recovery angles of fabrics treated with PUS-E1-5 and PUS-E2-5 were 136.9° and 148.5°, respectively; compared to fabrics treated with commercially available silicone softeners, the crease recovery angle of fabrics treated with biomimetic chain-extender samples was slightly improved. This is because the hydroquinone groups significantly enhanced the bonding strength between the additive and the fibers, enabling the polymer to form a uniform, stable, and moderately rigid softening film on the fiber surface, thereby effectively improving the fabric's wrinkle resistance.

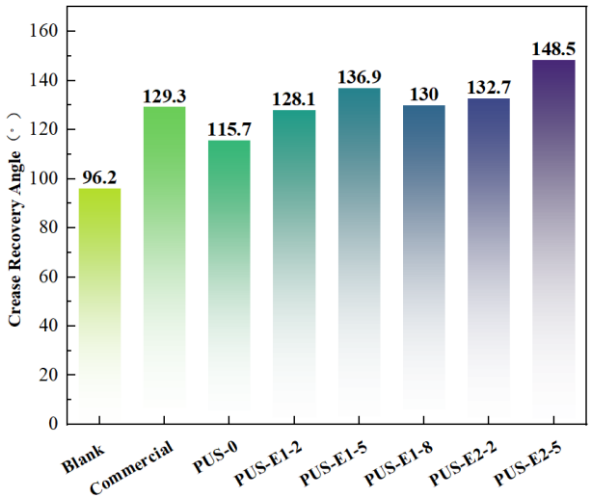


Fig. 4. Crease recovery angles of cotton fabrics treated with different PUS softeners

3.4.2. Flexibility

Polyurethane-modified polysiloxane polymer softeners reduce friction between fibers by forming a uniform, flexible, and smooth film on the fiber surface, thereby enhancing fabric softness [2]. As shown in Figure 5, before any washing, fabrics treated with PUS-E2-5 exhibit significantly better softness than fabrics treated with commercially available resin-type silicone softeners. With increasing wash cycles, the softness gradually decreases; however, after 30 washes, the fabric treated with the sample containing the monocatechol biomimetic chain extender (PUS-E1-5) still retains a softness of 201.4 mN, which is considerably lower than that of the commercial

product.

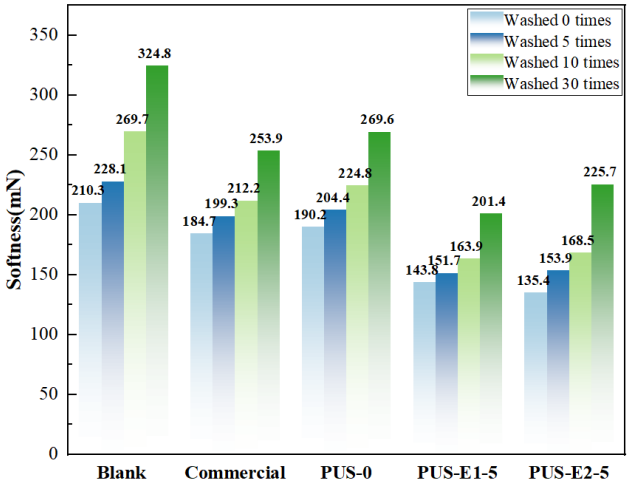


Fig. 5. Softness of cotton fabrics treated with different PUS softeners after repeated washing cycles

Furthermore, it is evident that the sample with the mono-catechol biomimetic chain extender (PUS-E1-5) has higher softness than the sample with the bis-catechol extender (PUS-E2-5) after 30 washes. This may be due to chain extension with CA_1-N_3 predominantly occurs at the more reactive amino groups, whereas the CA_2-N_3 extender has only one amino group readily available. Consequently, during chain extension, phenolic hydroxyl groups of CA_2-N_3 are consumed, resulting in weakened adsorption. In summary, the catechol group significantly enhances the adsorption of the silicone softener onto the fiber and its binding capacity, thereby significantly improving the softness and wash-fastness of the finished fabric.

3.4.3. Surface Morphology Analysis

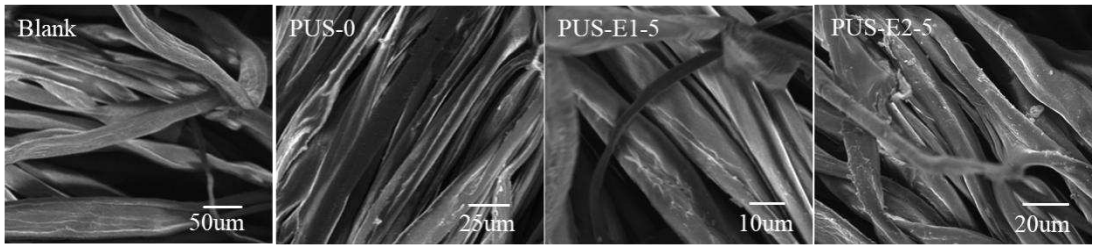


Fig. 6. SEM images of surface morphology of untreated and PUS-treated cotton fabrics

Surface morphology analysis was performed on fabric samples treated with PUS-E1-5, PUS-E2-5, and PUS-0, as well as on the untreated fabric. As shown in Figure 6, a distinct film structure was formed on the fiber surface after treatment with the PUS emulsion. In contrast, the fiber surface treated with the PUS-0 emulsion, which lacks the catechol group, exhibited minimal coating, and the fibers appeared relatively rough in the longitudinal direction illustrated that the introduction of the catechol structure in

the softener significantly enhances the adsorption and affinity, consistent with the strong affinity of phenolic hydroxyls for cellulose fibers[31]. This is manifested by a marked reduction in the roughness of the fiber surface, endowing the treated fabric with excellent softness and wash-fastness.

4. Conclusion

In this study, we successfully prepared and characterized amide-type polyurethane bionic chain extenders containing catechol groups (CA_1-N_3 and CA_2-N_3) through amidation reactions, and introduced them into the polyurethane-modified organosilicon softener backbone to create a series of resin-type organosilicon softeners. The catechol chain extenders significantly improved the thermal stability of the softeners while also enhancing the softness (135.4 mN) and elasticity (a crease recovery angle of 148.5°) of treated fabrics. More importantly, thanks to the strong adsorption and interfacial binding ability of the catechol groups to fibers, the softener forms a uniform and stable film on the fiber surface, keeping the fabric soft even after 30 times standard wash. This strategy effectively addresses the weak fiber binding and poor wash durability of traditional organosilicon softeners, providing a new technical approach for designing long-lasting softening finishes for high-end textiles and showing great potential for practical applications.

References

[1] D. Gupta, Softening treatments for technical textiles, Elsevier, 2013. https://doi.org/10.1533/9780857097613.2.154.

[2] L. Noor, U.B. Humayoun, N. Sarwar, A. Rasheed, D.H. Yoon, Towards a greener future: utilization of Citrullus colocynthis seed oil emulsion as sustainable functional soft finish for textiles application, Cellulose 31 (2024) 607-622. https://doi.org/10.1007/s10570-023-05608-8.

[3] Y. Song, W. Zhu, Q. Guo, Y. Li, H. Cen, Z. Xu, Synthesis of Cationic Waterborne Polyurethane-Polysiloxane Emulsion: Structure Regulation, Charge Compatibility Optimization, and Application in High-Performance One-Bath Softening–Dyeing Process, Journal of Applied Polymer Science 143 (2026). https://doi.org/10.1002/app.70159.

[4] S. Sezgin Bozok, R.T. Ogulata, Applying Softener Doped Silica Coating to Cotton Denim Fabrics, Journal of Natural Fibers 19 (2022) 7566-7578. https://doi.org/10.1080/15440478.2021.1952138.

[5] H.M. Fahmy, H.M.Y. Okda, A.G. Hassabo, M.H. El-Rafie, M.A. Youssef, Synthesis of New Silicone-based Adducts to Functionalize Cotton Fabric, Silicon 14 (2022) 7613-7621. https://doi.org/10.1007/s12633-021-01451-3.

[6] M. Zuber, K.M. Zia, S. Tabassum, T. Jamil, S. Barkaat-ul-Hasin, M.K. Khosa, Preparation of

rich handles soft cellulosic fabric using amino silicone based softener, part II: Colorfastness properties, International Journal of Biological Macromolecules 49 (2011) 1-6. https://doi.org/10.1016/j.ijbiomac.2011.01.025.

[7] Z. Huang, Q. Chen, W. Cheng, C. Li, M. Sun, L. Yu, Synthesis and characterization of a high-temperature resistant amino silicone softener for enhanced cotton fabric performance, Colloids and Surfaces A: Physicochemical and Engineering Aspects 711 (2025) 136415. https://doi.org/10.1016/j.colsurfa.2025.136415.

[8] H. Peng, P. Zhang, J. Xie, Z. Zhang, X. Cao, Properties of cotton fabrics treated by etherification and esterification and esterification/addition crosslinking with an amino-functional silicon softener, Cellulose 28 (2021) 7341-7354. https://doi.org/10.1007/s10570-021-03961-0.

[9] J.J. Chruściel, Modifications of Textile Materials with Functional Silanes, Liquid Silicone Softeners, and Silicone Rubbers—A Review, Polymers 14 (2022) 4382. https://doi.org/10.3390/polym14204382.

[10] W. Lei, Y. Sun, B. Huang, X. Zhou, Synthesis and Application of Polyurethane-Modified Silicone as Finishing Agent for Cotton Fabric, Fibers and Polymers 19 (2018) 1024-1031. https://doi.org/10.1007/s12221-018-7931-7.

[11] Y. Wu, Y. Sun, K. Chen, Y. Hong, X. Zhou, Synthesis and application of silicone-modified polyurethane as a slip-elastic finishing agent for polyamide fabrics, Progress in Organic Coatings 191 (2024) 108420. https://doi.org/10.1016/j.porgcoat.2024.108420.

[12] H.S. Cho, H.J. Yoon, B.H. Lee, J.C. Woo, H.Y. Choi, E. Shim, J.H. Youk, Evaluation of Touch and Durability of Cotton Knit Fabrics Treated with Reactive Urethane-Silicone Softener, Polymers 14 (2022) 1873. https://doi.org/10.3390/polym14091873.

[13] K.T. Rashid, N. Akram, K.M. Zia, M. Usman, Biobased monomers based textile finishing: A new approach to improving poly/cotton fabrics by waterborne polyurethane dispersions, International Journal of Biological Macromolecules 306 (2025) 141424. https://doi.org/10.1016/j.ijbiomac.2025.141424.

[14] H.-L. Li, Z.-S. Jiang, F. Wang, R.-G. Zhang, R.-Y. Sun, Y.-Z. Wang, F. Song, Alkyl Side-chain Engineering for Enhanced Anti-wettability and Stability in Non-fluorinated Liquid-repellent Coatings, ACS Applied Materials & Interfaces 17 (2025) 48863-48872. https://doi.org/10.1021/acsami.5c08629.

[15] W. Lai, B. Qin, X. Cao, Q. Chen, J.-F. Xu, X. Zhang, Supertough and Multirecyclable Cross-Linked Polyurethane Enabled by Supramolecular Chain Extenders and Noncovalent Cross-Linkers, Journal of the American Chemical Society 147 (2025) 29517-29525. https://doi.org/10.1021/jacs.5c10178.

[16] P. Huang, H. Zhang, H. Zeng, Mussel-Inspired Molecular Strategies for Fabricating Functional Materials With Underwater Adhesion and Self-Healing Properties, Advanced Materials 37 (2025). https://doi.org/10.1002/adma.202501542.

[17] X. Wang, Y. He, B. Cui, Y. Feng, J. Lin, X. Long, Y. Wang, Z. Li, F. Luo, J. Li, H. Tan, Catechol-induced assembly to enhance the performance of antimicrobial peptide fully, Chemical Engineering Journal 524 (2025) 169195. https://doi.org/10.1016/j.cej.2025.169195.

[18] W. Wang, J. Liu, S. Zhu, C. Wang, Y. Li, X. Leng, A Mussel-Inspired Design for Robust Catechol-Functionalized Cross-Linking Adhesives Uniting Water Resistance, Low-Temperature Stability, Recyclability, Degradability, and Fluorescence, ACS Applied Materials & Interfaces 17 (2025) 43645-43654. https://doi.org/10.1021/acsami.5c09120.

[19] F. Yan, G. Wang, S. Dai, Q. Huang, G. Su, X. Zhan, L. Liu, Bio-Based Waterborne Polyurethane Sizing Agent Containing Strong Adhesion Catechol Structure for the Interfacial Enhancement of Carbon Fiber/Polyamide 6 Composites, Polymer Composites 47 (2026) 6643-6652. https://doi.org/10.1002/pc.70581.

[20] S. Inata, H. Sogawa, F. Sanda, Water-soluble alginate–based adhesive: catechol modification and adhesion properties, Polymer Journal 55 (2023) 785-795. https://doi.org/10.1038/s41428-023-00770-z.

[21] M. Xiao, L. Deng, J. He, Y. Xu, S. Liu, H. Lin, N. Qi, D. Zhang, Bioinspired Catechol-PEG Functionalized PVDF Nanofiber Membranes with Hydrophilicity-Adhesion Synergy for Reliable Skin-Conformal Sweat Sensing, ACS Applied Materials & Interfaces 17 (2025) 51144-51154. https://doi.org/10.1021/acsami.5c11437.

[22] J. Lou, R. Sun, J. Yuan, J. Xu, X. Fan, Z. Gu, In-situ polymerization, colorization, and functionalization of amino-modified cotton fabrics with Catechol via horseradish peroxidase-hydrogen peroxide system, Cellulose 31 (2024) 4581-4595. https://doi.org/10.1007/s10570-024-05859-z.

[23] X. Yu, Y. Xiong, Z. Li, H. Tang, Preparation and Characterization of Tris(trimethylsiloxy)silyl Modified Polyurethane Acrylates and Their Application in Textile Treatment, Polymers 12 (2020) 1629. https://doi.org/10.3390/polym12081629.

[24] Y. Wu, Y. Sun, K. Chen, Y. Hong, X. Zhou, Synthesis and application of silicone-modified polyurethane as a slip-elastic finishing agent for polyamide fabrics, Progress in Organic Coatings 191 (2024) 108420. https://doi.org/10.1016/j.porgcoat.2024.108420.

[25] F.S. Chuang, W.C. Tsen, Y.C. Shu, The effect of different siloxane chain-extenders on the thermal degradation and stability of segmented polyurethanes, Polymer Degradation and Stability 84 (2004) 69-77. https://doi.org/10.1016/j.polymdegradstab.2003.10.002.

[26] J. Yeh, Y. Shu, Characteristics of the degradation and improvement of the thermal stability of poly(siloxane urethane) copolymers, Journal of Applied Polymer Science 115 (2010) 2616-2628. https://doi.org/10.1002/app.29023.

[27] M. Takamura, T. Nakamura, T. Takahashi, K. Koyama, Effect of type of peroxide on cross-linking of poly(l-lactide), Polymer Degradation and Stability 93 (2008) 1909-1916. https://doi.org/10.1016/j.polymdegradstab.2008.07.001.

[28] P. Honcová, R. Svoboda, J. Málek, Influence of sample form and thermal history on relaxation response, Thermochimica Acta 507–508 (2010) 71-76. https://doi.org/10.1016/j.tca.2010.05.003.

[29] A. Serrano-Lotina, R. Portela, P. Baeza, V. Alcolea-Rodriguez, M. Villarroel, P. Ávila, Zeta potential as a tool for functional materials development, Catalysis Today 423 (2023) 113862. https://doi.org/10.1016/j.cattod.2022.08.004.

[30] H. Mao, Y. Gao, W. Chen, Y. Hong, Y. Sun, Synthesis and application of polyurethane-modified silicone softener for enhanced fabric softness and elasticity, Progress in Organic Coatings 197 (2024) 108864. https://doi.org/10.1016/j.porgcoat.2024.108864.

[31] Z. Tang, X. Lin, M. Yu, J. Yang, S. Li, A.K. Mondal, H. Wu, A review of cellulose-based catechol-containing functional materials for advanced applications, International Journal of Biological Macromolecules 266 (2024) 131243. https://doi.org/10.1016/j.ijbiomac.2024.131243.

CRediT authorship contribution statement

Heng Quan: Writing – original draft, Software. **Bing Wu:** Writing –review & editing. **Qinglin Fu:** Investigation. **Lijie Ni:** Writing – review & editing. **Li Xiao:** Investigation, Data curation. **Zengfeng Wei:** Writing – review & editing, Supervision, Funding acquisition.

Declaration of Competing Interest

No potential conflict of interest was reported by the authors.

Data Availability

Data will be made available on request.

Acknowledgements

The author sincerely thanks the Science and Technology Department of Xinjiang Uygur Autonomous Region for providing financial support for the "Salt-Free Dyeing Technology for Cellulose Fibers with Active Dyes" project in the first batch of the 2024 "Challenge-Based" program, as well as the 2025 Jingzhou City Challenge-Based Science and Technology Project (Project Number 2025JA07).